RSC Advances

PAPER

View Article Online
View Journal | View Issue

Cite this: *RSC Adv.*, 2021, **11**, 17611

Synthesis and antioxidant activities of berberine 9-*O*-benzoic acid derivatives†

Yanfei Liu,[a] Shuo Long,[a] Shanshan Zhang,[a] Yifu Tan,[a] Ting Wang,[b] Yuwei Wu,[b] Ting Jiang,[a] Xiaoqin Liu,[a] Dongming Peng[c] and Zhenbao Liu*[b]

Received 18th February 2021
Accepted 17th April 2021

DOI: 10.1039/d1ra01339d

rsc.li/rsc-advances

Although berberine (**BBR**) shows antioxidant activity, its activity is limited. We synthesized 9-*O*-benzoic acid berberine derivatives, and their antioxidant activities were screened *via* ABTS, DPPH, HOSC and FRAP assays. The *para*-position was modified with halogen elements on the benzoic acid ring, which led to an enhanced antioxidant activity and the substituent on the *ortho*-position was found to be better than the *meta*-position. Compounds **8p**, **8c**, **8d**, **8i**, **8j**, **8l**, and especially **8p** showed significantly higher antioxidant activities, which could be attributed to the electronic donating groups. All the berberine derivatives possessed proper lipophilicities. In conclusion, compound **8p** is a promising antioxidant candidate with remarkable elevated antioxidant activity and moderate lipophilicity.

1. Introduction

Berberine (**BBR**), a natural isoquinoline alkaloid isolated from *Coptis chinensis* and *Hydrastis canadensis*,[1] has proved to possess activity for various diseases, such as inflammation,[2] diabetes,[3] insulin resistance, Alzheimer's disease, acute endotoxemia,[4] and maintenance of the gut mucosal barrier function[5] with intestinal transport ability.[6] It has been confirmed that the inhibitory effect of **BBR** on oxidative stress was observed both in cells and animal models, which were associated with oxidative stress.[7] In addition, the excessive accumulation of ROS is attributed to the imbalance between the antioxidant defense systems and production of reactive oxygen species (ROS), including superoxide anion ($O^{2-\bullet}$), hydroxyl radical ($OH^{\bullet}$), and hydrogen peroxide (H_2O_2), leading to oxidative stress, which is a key factor of metabolic disorder, acute respiratory distress syndrome,[8] idiopathic pulmonary fibrosis,[9] neurodegenerative disorders, insulin resistance, acceleration of the aging process,[10–12] impairing of the DNA repair systems[13] and inducing apoptosis of the pancreatic islet β-cells.[14]

Although accumulating evidence has shown the usefulness of **BBR** in reducing oxidative stress,[15] its antioxidant activity is not effective enough compared with other synthetic antioxidant agents, which play a dominant role in clinical use. **BBR** derivates, containing phenolic hydroxy groups, have been reported with enhanced antioxidant activity. At the same time, 8-oxocoptisine,[16] indole,[17] piperazine[18] and benzothiazole[19] derivatives of berberine have also been developed in recent years, while the C-9 position modification of benzoic acid was seldom reported. In our previous work, we designed and synthesized a series of berberine derivatives, and demonstrated that the introduction of an aromatic nucleus on the C-9 position of berberine had important influences on hypoglycemic[20] and anti-inflammatory activities,[21] which were closely related with oxidative stress. Because antioxidant activation is closely related to the electric potential distribution,[22] introducing electron-donating groups on the aromatic nucleus is a frequent approach for achieving improved antioxidant activity. Therefore, we synthesized a series of berberine-aromatic derivatives with electron-donating groups, such as methoxy, methyl and acetoxyl groups (compounds **8a–8p**), modified on the C-9 position. We further screened their antioxidant activities by ABTS, DPPH, HOSC and FRAP assays, and comprehensively analyzed the results *via* color grading profiles.

2. Results and discussion

2.1. Synthesis

Compounds in this study were prepared according to Scheme 1. Compound **2** containing an acetoxyl group was obtained by alkylation of the phenolic hydroxyl group of compound **1** with acetic anhydride in the presence of phosphoric acid at 90 °C for 5–10 min. Compound **3** was synthesized from compound **1**, containing the phenolic hydroxyl group by treatment with dimethyl sulfate in sodium hydroxide solution for 4.5 h according to the literature.[23] The leading compound (berberine, **6**) was demethylated on the 9-O position, following a previously described method.[24] In simple terms, it was heated at 190 °C in a dry oven under vacuum (20–30 mmHg) for 0.5–1 h to obtain a dark red solid, and purified by recrystallization from methyl

[a]*Department of Pharmaceutical Engineering, College of Chemistry and Chemical Engineering, Central South University, Changsha, 410083, China*

[b]*Department of Pharmaceutics, Xiangya School of Pharmaceutical Sciences, Central South University, Changsha, 410013, China. E-mail: zhenbaoliu@csu.edu.cn*

[c]*Department of Medicinal Chemistry, School of Pharmacy, Hunan University of Chinese Medicine, Changsha, 410208, China*

† Electronic supplementary information (ESI) available. See DOI: 10.1039/d1ra01339d

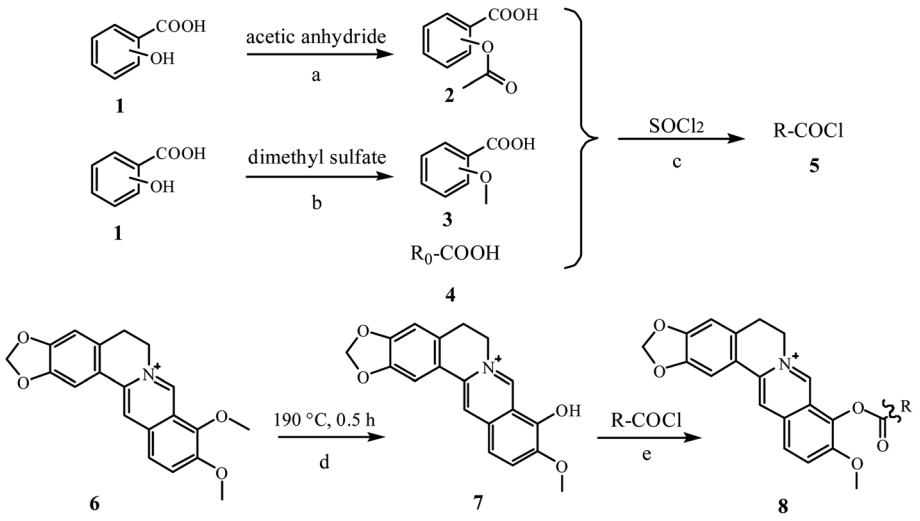

8a-8p: R=

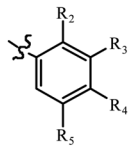

Compounds	R_2	R_3	R_4	R_5
8a	H	H	H	H
8b	OCH_3	H	H	H
8c	OCH_3	H	H	Cl
8d	OCH_3	H	H	Br
8e	H	H	OCH_3	H
8f	OEt	H	H	H
8g	OAc	H	H	H
8h	OAc	H	Cl	H
8i	OAc	H	H	Cl
8j	OAc	H	H	Br
8k	OAc	H	CH_3	H
8l	OAc	H	H	CH_3
8m	H	H	OAc	H
8n	H	OCH_3	OCH_3	OCH_3
8o	H	OEt	OEt	OEt
8p	H	OAc	OAc	OAc

Scheme 1 Synthetic procedure and chemical structures of berberine derivatives. Reagents and conditions: (a) acetic anhydride, H_3PO_4, room temperature; (b) dimethyl sulfate, NaOH, 95–100 °C, 2 h; (c) $SOCl_2$, pyridine, 75 °C, 1–2 h; (d) vacuum (20–30 mmHg), 190 °C, 0.5–1 h; (e) pyridine, acetonitrile, room temperature, 2–4 h.

alcohol to obtain berberrubine (**7**). The benzoic acid derivatives (**2**, **3**, **4**) were treated by thionyl chloride, then condensed with berberrubine **7** in the presence of pyridine to obtain compound (**8**). The compounds were purified by recrystallization with methanol. Structures of all of the synthesized berberine derivatives were explicitly characterized by IR, ^{1}H NMR, and HRMS.

2.2. Log *P*

The results are summarized in Table 1. Generally, moderate lipophilicity (log P = 0–3) is benefit to the druggability of drug candidates. As we expected, the lipophilicities of the synthesized compounds were increased compared with that of berberine. It is noteworthy that the values of log P of the berberine derivatives were in a range from 1.23 to 2.13. Usually, the compounds with log P of between 0–3 have good gastrointestinal absorption, indicating the synthesized compounds met the requirements for oral administration.[25] The different log P may also lead to diverse antioxidant activities.

2.3. Antioxidant activities evaluation

2.3.1. ABTS assay. As shown in Fig. 1, **BBR** derivatives showed diverse abilities in scavenging ABTS radicals, and most of their abilities were greater than that of **BBR**, which may have resulted from the enhancement of lipophilicity *via* esterification

Table 1 Log P values of berberine and berberine derivatives

Compounds	Log P	Compounds	Log P
BBR	−0.18	**8i**	1.46
8a	1.23	**8j**	1.41
8b	1.29	**8k**	1.56
8c	1.71	**8l**	1.56
8d	1.83	**8m**	1.24
8e	1.31	**8n**	1.27
8f	1.66	**8o**	2.06
8g	1.24	**8p**	2.13
8h	1.67		

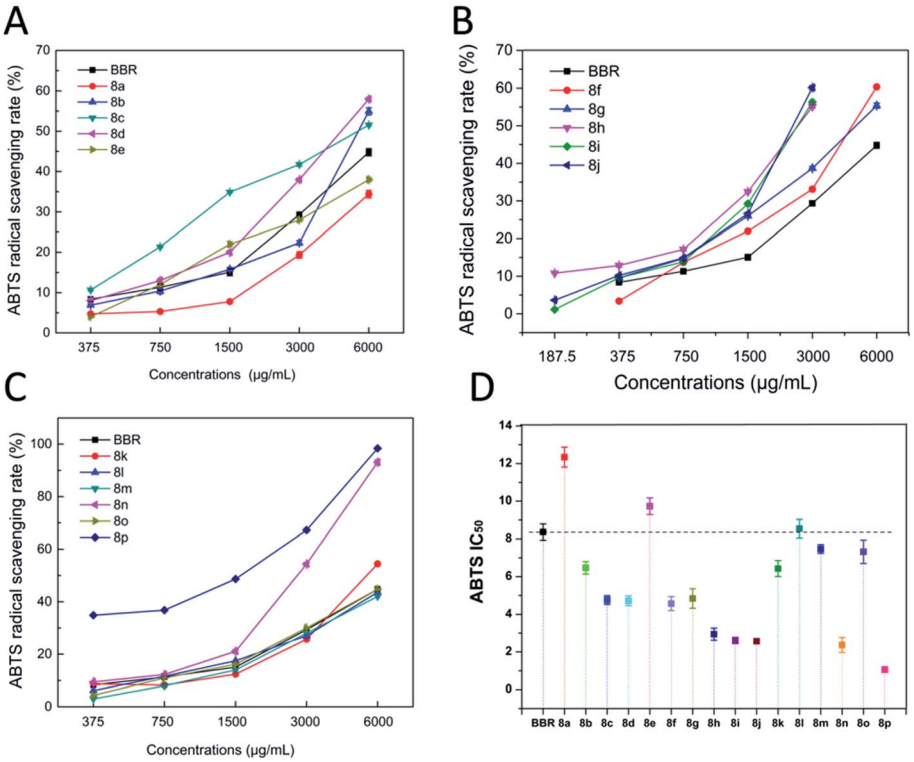

Fig. 1 ABTS radical scavenging capacities (A–C) and IC_{50} (D) of berberine derivatives.

process and the incorporation of aromatic acid. Compared with **BBR**, compounds **8h**, **8i**, **8j** and **8n**, **8p**, with the IC_{50} values ranging from 1.06 ± 0.15 to 2.94 ± 0.32 mg mL^{-1}, exhibited superior efficacy in radicals scavenging (3–8-fold). Among them, compounds **8c**, **8d**, **8f**, and **8g** had moderate antioxidant capacities, while **8b**, **8k**, **8m**, and **8o** showed slightly higher antioxidant capacities, and compounds **8a** and **8e** exhibited lower antioxidant capacities.

The ABTS assay is an electron-transfer-based assay that measures the capacity of an antioxidant in reducing the oxidants. Among

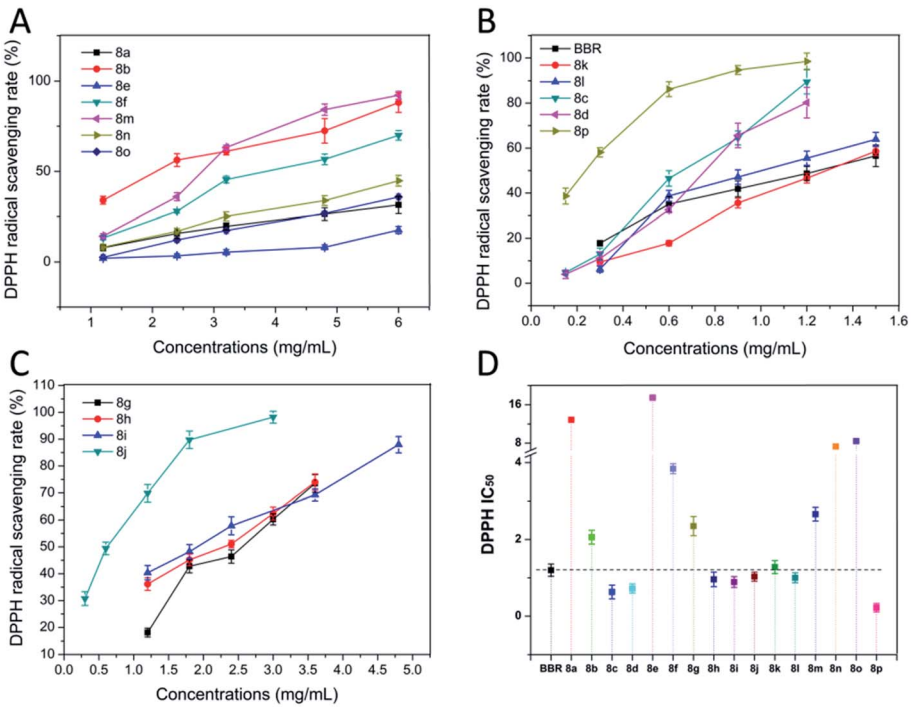

Fig. 2 The DPPH radical scavenging capacities (A–C) and the IC_{50} (D) of **BBR** and **BBR** derivatives.

these compounds, there is a correlation between the structure and radical-scavenging capacities. Compound **8a** showed the lowest capacity, and this may be attributed to the introduction of electron-donating groups, which was accordance with the research conducted by Bhupendra Mistry.[17] To investigate the relationship between different substituents and scavenging capacities, compound **8a** was used as a basic compound. It was found that the compounds possessing an aromatic nucleus showed enhanced antioxidant capacities, which could be attributed to the oxygen-containing moieties. The position of the substituent is also an influence factor. Different positions of the same substituents exhibited different capacities, especially at the *para*-position. The activation of radical scavenging involves increased stabilization of radicals and other electron deficient intermediates, which are formed during oxidation.[26] Therefore, the introduced electron-donating groups were beneficial to the reducing of the antioxidant activity, which may be attributed to the electronic effect contributed to the free radical reaction on benzene.

Compounds **8g** and **8f** showed enhanced antioxidant capacities. The benzoic acid with acetoxyl substitution derivatives (compounds **8g**, **8i**, **8j**) were more efficient than their methoxy substitutes (compounds **8b**, **8c**, **8d**). With regard to the aromatic substitution, the order of effectiveness was acetoxy group (compound **8g**) ≈ ethoxy group (compound **8f**) > methoxy group (compound **8b**) > hydrogen group (compound **8a**). The activity of **8i** > **8c** and **8j** > **8d**, indicated that the acetoxyl group (–$OCOCH_3$) substitution contributed superior antioxidant activity compared to that of the methoxy group (–OCH_3) substitution. We also found that when the benzene rings contain halogens, the antioxidant activities of the compounds will be significantly improved, as shown by the activities of **8c**, **8d**, **8h**, **8i** and **8j** compared to that of **8b**. The R_2 position substituent contributed more to the activity than the R_4 position, as confirmed by the activities of **8b** > **8e**, and **8g** > **8m**. The substituent acetoxyl (–$OCOH_3$) can provide better antioxidant activity compared with methoxyl (–OCH_3), as indicated by the activities of **8e** < **8m**, **8c** < **8i**, and **8d** < **8j**.

2.3.2. DPPH assay. As shown in Fig. 2, **8h**, **8j**, **8l** have similar activities with **BBR**. **BBR** and its derivatives possessed scavenging capacities for DPPH radicals. The activities of compounds **8c**, **8d**, **8i**, **8p**, and especially, **8c**, **8d**, **8p** were better than that of **BBR** at the concentration of 1.2 mg mL^{-1}, and the radical scavenging ratio of **8c**, **8d**, **8p** reached 80%, 85%, and 97% (Fig. 2B), respectively, while **BBR** is only 50%. Compound **8p** was 6 times compared to **BBR**. In contrast, compounds **8a**, **8b**, **8e**, **8f**, **8g**, **8m**, **8n**, **8o**, and especially **8a**, **8e** exhibited lower scavenging activities than **BBR**. The replacement of hydrogen on the aromatic ring by a halogen atom or methyl group donated enhanced activities (compounds **8c** and **8d** > **8b**, compounds **8i** and **8j** > **8g**). Aside from the aromatic substitution, the position of the substitution has significant influences on the activities. *Para*-methoxy- (compound **8e**) and *para*-acetoxyl- (compound **8m**) benzoic

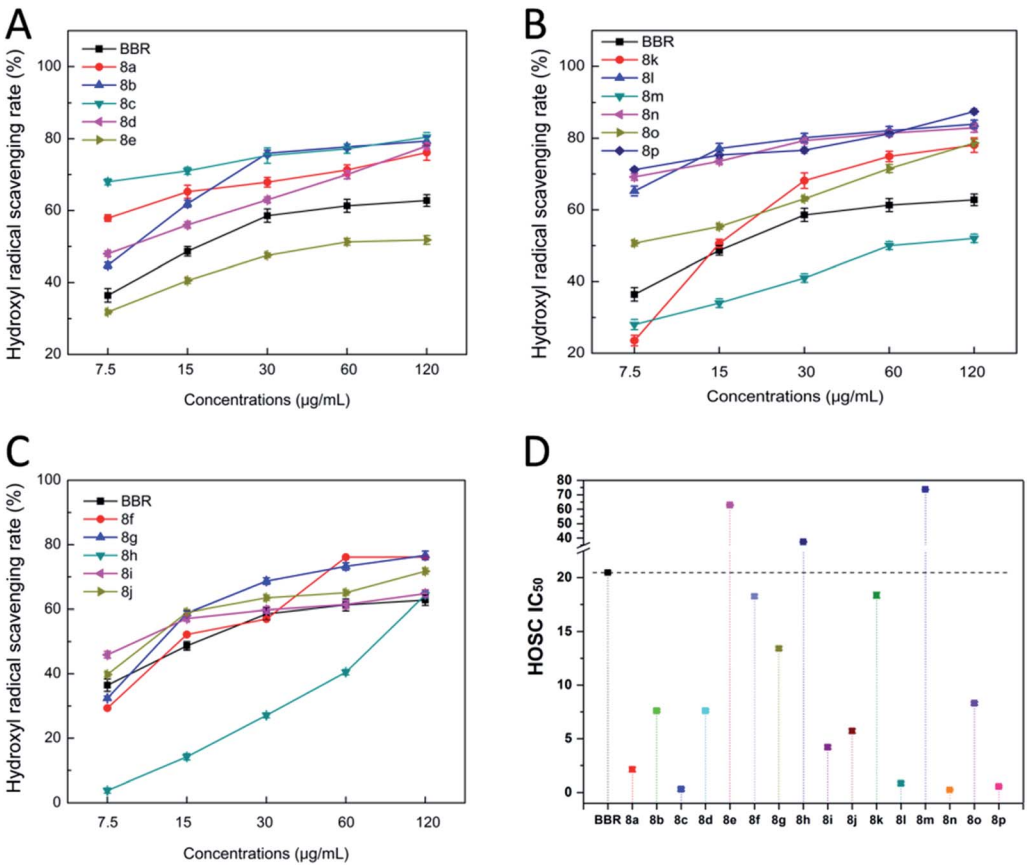

Fig. 3 The hydroxyl radical scavenging capacities (A–C) and the IC_{50} (D) of **BBR** and **BBR** derivatives.

acid berberine derivatives showed lower antioxidant ability than their *ortho*-substitutes (compounds **8b** and **8g**), respectively.

2.3.3. HOSC assay. Most of the derivatives showed higher values than **BBR** (Fig. 3). The IC_{50} values range from 0.25 ± 0.06 to 73.70 ± 0.11 μg mL^{-1} compared with **BBR** (20.48 ± 0.14 μg mL^{-1}). Among them, compounds **8c**, **8l**, **8n** and **8p** exhibited better antioxidant activities, while compounds **8e**, **8m**, and **8h** showed poorer activities. This assay again showed that the *para*-substitution had a negative effect on the antioxidant activity (compounds **8l** > **8k**, **8h** < **8i**, indicating that the R_5 position was better than the R_4 position for a substituent; compounds **8b** > **8e**, **8g** > **8m**, indicating that the R_2 position substituent was better than the R_4 position substituent). Compound **8j** > **8d**, indicating that the acetoxyl (–$OCOCH_3$) substituent was better than the methoxy (–OCH_3) substituent. Compound **8p** exhibited significantly enhanced activity, which was in accordance with other antioxidant assays.

2.3.4. FRAP assay. As shown in Fig. 4, these results showed that all the tested compounds exhibited a ferric reducing power. Furthermore, most of the modified compounds, especially **8i**, **8j**, **8p**, exhibited significantly higher activities than its natural precursor (**BBR**). When the concentration reached 187.5 μg mL^{-1}, the reducing capacities increased by 10, 10 and 40 times, respectively, compared to **BBR**, while others, such as **8e**, **8f**, **8h** and **8m**, possessed a similar or slight decrease in the Fe(II) equivalent. Fig. 4D shows that at the same concentration of 187.5 μg mL^{-1}, compound **8p** possessed dramatically enhanced antioxidant capacity (421.50 ± 0.77 μM), which is nearly 50 times greater than that of **BBR** (8.81 ± 0.36 μM). We also found that having substituent halogens at the R_5 position was better than the methyl (–CH_3) group due to the fact that **8c** > **8b**, **8d** > **8b**, **8i** ≫ **8g**, **8j** ≫ **8g**, **8i** > **8l**, **8j** > **8l**. The acetoxyl (–$OCOCH_3$) substituent was better than the methoxy (–OCH_3) substituent, as further confirmed by the activities of **8g** > **8b**, **8i** > **8c**, **8j** > **8d**, and **8m** > **8e**.

These results proved that there were regularities between the ferric reducing power and the substituents on benzene. Compounds introducing a benzene ring with an acetyl oxygen substituent possessed potent ferric reducing capacities that were greater than that modified with the methoxyl substituent. In addition, replacing the hydrogen atom with oxygen-containing moieties on the *ortho*-position of benzene donated reduced activities.

Based on the above experimental data, we speculated that the introduction of an electron-donating group on the benzene ring could increase its electron cloud density, and the electric effect was beneficial to the free radical reaction of benzene, thereby increasing the antioxidant activity to some degree. Furthermore, the effectiveness was acetoxy group > methoxy group, and this may be related to their electron-donating abilities. At the same time, we also found that the substitutes at the *ortho*-position had a positive effect on the antioxidant activity, and the substitutions at the *para*-position hindered the antioxidant activity to some extent. Having a substituent at the *ortho*-position, and introduction of a halogen or a methyl group at the *meta*-position can also enhance the antioxidant activity. Moreover, it was better to have multiple substituents on the benzene ring than to have only one substituent.

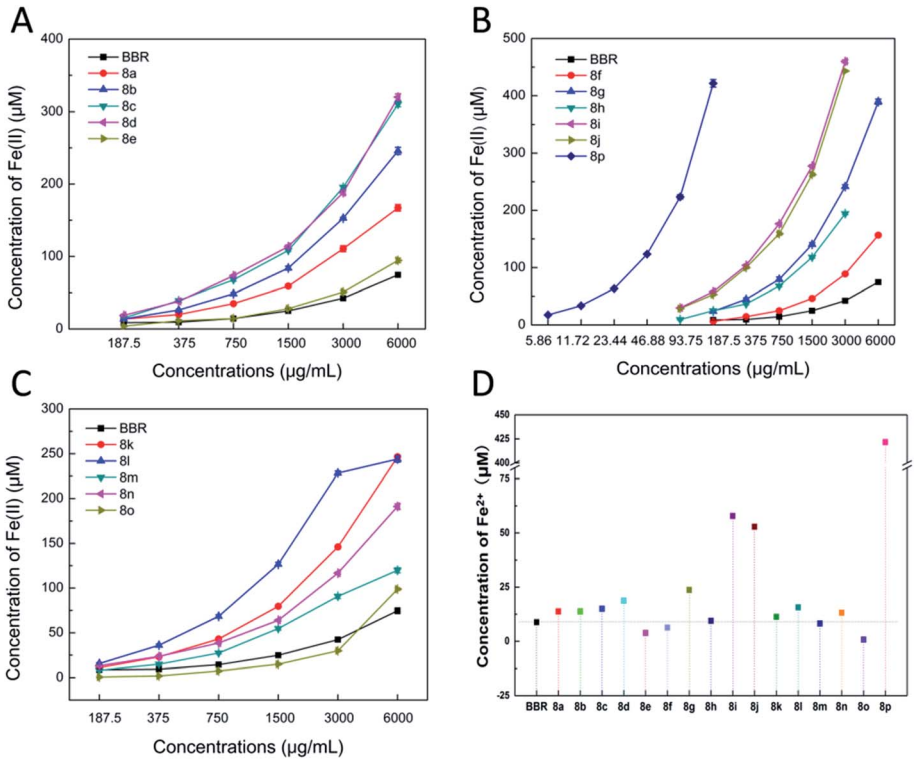

Fig. 4 (A–C) The Fe^{3+} reducing capacities of **BBR** and **BBR** derivatives. (D) The Fe^{3+} reducing capacities of **BBR** and **BBR** derivatives at a concentration of 187.5 μM.

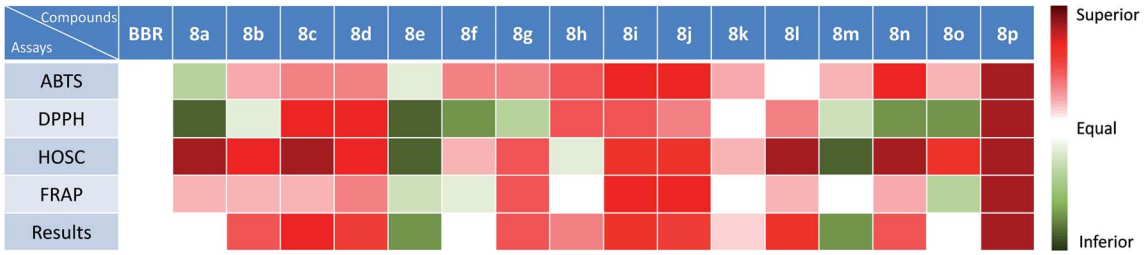

Fig. 5 Comprehensive analysis of the antioxidant activities using the color grading profile.

2.4. Comprehensive analysis of the antioxidant activity using color grading profile

The results from different assays resulted in different results, which may be attributed to the fact that the detection principles were different, and thus led to differentiation. However, most of the compounds showed similar results from the four assays. From the results (a mixture color of the result color from four assays) in Fig. 5, we can find that compounds **8p**, **8c**, **8d**, **8i**, **8j**, and **8l** showed significant enhanced activities, and compounds **8b**, **8g**, **8h**, **8n**, and **8k** showed slightly increased activities. Compounds **8a**, **8f**, and **8o** showed equal activities with **BBR**, and compounds **8e**, **8m** showed lower activity.

2.5. The relation of the molecular electrostatic potentials (MEPs) with the antioxidant activity

As shown in Fig. 6, the ESP distribution color at the position of the berberine methylenedioxy group, which is the pharmacophore of the antioxidant, was close to red, indicating that this position has the trend of donating electrons. Compared with **BBR** in Fig. 6A, compound **8p** in Fig. 6B exhibited a more extensive red area on the introduced groups at the C-9 and acetoxyl groups. Thus, it can be considered that the trend of donating electrons in compound **8p** was more obvious compared with berberine, which was in accordance with the dramatically enhanced antioxidant activity.

N-Acetyl-L-cysteine, which can increase the GSH concentration in the lungs by supplementing L-cysteine with the GSH precursor protein, has been shown to reduce ROS and reduce airway inflammation and AHR by regulating activation of NF-κb and HIF-1α.[27,28] *N*-Acetyllysine (Nal), which reduced the ROS levels and inflammatory responses, showed an IC_{50} value of the antioxidation activity at 290 μm.[29] γ-Glutamylcysteine, a precursor of glutathione, could enter cells to suppress LPS-induced inflammation, prevent ROS accumulation and GSH depletion.[30] Clinical trials have shown that oral administration of γ-glutamylcysteine increases the intracellular glutathione levels above homeostasis.[31] Ebselen protected peroxynitrite in a dose-dependent manner, and its EC_{50} value is 8.0 μm.[32] It is a promising candidate for treatment of COVID-19 and other respiratory virus infections.[33] Ergothionine (EGT) inhibited liposome oxidation by 67% and 100% at 20 μm and 100 μm, respectively,[34] which showed similar antioxidant activity to coenzyme Q10. Polyphenols represent antioxidant natural products from a variety of plant sources, and gallic acid has been shown to be effective in scavenging free radicals. A DPPH assay showed that gallic acid, which consumed free radicals through a hydrogen-donating mechanism, was more effective than vitamin E.[35] Resveratrol and its derivatives play important roles in scavenging H_2O_2 and inhibiting oxidative stress by activating the antioxidation mechanism of Keap-1/Nrf2, as shown in an asthma rat model, and have potential value as functional food additives.[36,37]

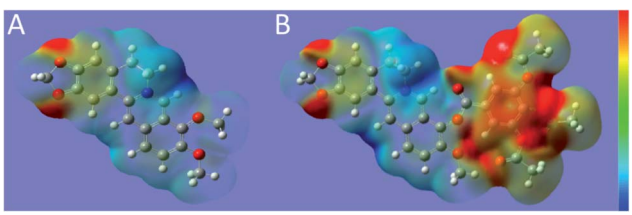

Fig. 6 The MEPs distribution maps of (A) **BBR** and (B) compound **8p**. The molecular electrostatic potential distribution of the charge density was presented by a color code from red to blue (from 0.05 to 0.143 hartree).

In contrast, the lipophilic berberine was effective in inhibition against lipid peroxidation and in protecting rat hepatocytes from oxidative stress.[38] The scavenging activity of the hydroxyl radical of berberine and its metabolite was 23% and 85% at 1 mM concentration, respectively. The hydroxy group at the C-9 position of berberine and its derivative played an important role in the scavenging activity.[39] Moreover, berberine protected mice from LPS-induced oxidative damage and improved the survival rate of mice.[40] In addition, berberine has been shown to be able to scavenge a variety of free radicals, which is may be related to the involvement of berberine in the redox reaction.[41] Experiments using DPPH, ABTS radical scavenging, nitric oxide scavenging, lipid peroxidation and other radical scavenging methods compared berberine and vitamin C. It was found that berberine showed antioxidant activity which was comparable to vitamin C, and displayed a variety of mechanisms to achieve the anti-oxidation effect, which proved the potential of berberine in anti-oxidation therapy.[41] In summary, the synthesis and exploration of berberine-based derivatives has great potential and good prospects in the treatment of reactive oxygen species-related diseases, such as asthma and cytokine storms.

In this work, a series of 9-*O*-benzoic acid substituted berberine derivatives were synthesized and their antioxidant activities were evaluated by DPPH, ABTS, FRAP and HOSC

assays. The antioxidant activities were not judged based on a single test, but a comprehensive assessment by a series of assays. According to the results of DPPH, ABTS, FRAP and HOSC, compounds **8p**, **8c**, **8d**, **8i**, **8j**, and **8l** showed superior antioxidant activity compared with **BBR**. In particular, compound **8p** can be used as a potential antioxidant, which had 6 times, 8 times and 36 times greater radical scavenging capacities in DPPH, ABTS and HOSC assays, respectively, and 48 times greater ferric ion reducing antioxidant power compared with that of **BBR**. This compound may be a potential drug for the treatment of the reactive oxygen species (ROS)-related diseases, such as the treatment of cytokine storms which are critical clinical conditions induced by the ROS in the pathogenesis of COVID-19.

3. Experimental

3.1. General experimental procedures

The ^{1}H NMR spectra were recorded on Bruker Avance III 500 MHz and Avance III 400 MHz NMR spectrometers from Bruker (Karlsruhe, Germany), respectively, with tetramethylsilane (TMS) as the internal standard. The IR spectra were measured by a Nicolet 6700 FTIR spectrometer from Thermo Fisher Scientific (Boston, MA, USA). Samples were ground with KBr and compressed to pellets. The HRMS were measured by a Water XEVO G2-XS QT high-resolution mass spectrometer from Waters (Boston, MA, U.S.A.).

3.2. Material

Berberine chloride was purchased from Lion Biological Technology (Zhengzhou, China). Benzoic acid, salicylic acid and other chemical raw materials were purchased from Bide Pharmatech, Ltd. (Shanghai, China). 1,1-Diphenyl-2-trinitrophenylhydrazine (DPPH), 2,2′-azinobis-(3-ethylbenzothiazoline-6-sulfonic acid) diammonium salt (98%) (ABTS) and 2,4,6-tri-(2-pyridyl)-1,3,5-triazine (TPTZ) were from Aladdin (Shanghai, China). Other commonly used reagents were from Sinopharm Chemical Reagent Co., Ltd. (Shanghai, China).

3.3. Synthesis of berberine derivatives

3.3.1. Synthesis of compound 2. Taking salicylic acid as example, a mixture of salicylic acid (2.0 g, 0.015 mol) and acetic anhydride (5 mL, 0.05 mol) was added to a flask, and phosphoric acid (5–7 d) was dropped into the mixture under stirring. Then, the mixture was stirred for 5–10 min at 90 °C. Finally, the mixture was cooled to room temperature to obtain white crystals.

3.3.2. Synthesis of compound 3. Taking salicylic acid as an example, a solution of 8 g sodium hydroxide in 47 mL water was cooled to 0 °C, and 0.1 mol salicylic acid was added under stirring. 10 mL dimethyl sulfate was quickly added under cool condition, and the mixture was heated to 35 °C and stirred for 20 min at 35 °C. An additional 10 mL of dimethyl sulfate was added. The mixture was stirred for 10 min at 45 °C, heated to 95–100 °C, and stirred for 2 h at 95–100 °C. A solution of 3.9 g NaOH in 13.3 mL water was added, and the mixture was stirred for 2 h at 95–100 °C. The mixture was cooled to room temperature, and 2 mL concentrated hydrochloric acid was added until the pH value changed to 1. The mixture became turbid, and the product was extracted with diethyl ether. Removal of the solvent from the extract gave 2-methoxybenzoic acid.

3.3.3. Synthesis of compound 5. Taking benzoic acid as an example, a solution containing benzoic acid (3.7 g, 0.03 mol) and pyridine (3 d) in dry $SOCl_2$ (3–10 mL) was heated at 75 °C for 1–2 h under nitrogen atmosphere. Then, the reaction mixture was concentrated under reduced pressure to give benzoyl chloride.

3.3.4. Synthesis of compound 7. Berberine chloride (**6**) (16.8 g, 0.05 mmol) was heated at 190 °C in a dry oven under vacuum (20–30 mmHg) for 0.5–1 h to obtain a dark red solid. It was purified by recrystallizing from methyl alcohol to obtain berberrubine (7).

3.3.5. Synthesis of compound 8. Taking benzoic acid (3.7 g, 0.03 mol) as an example, benzoyl chloride was added to the solution of berberrubine (7) (3.86 g, 0.012 mol) in 40 mL acetonitrile and 4 mL pyridine, stirred for 2–4 h at room temperature, and the reaction was monitored by thin-layer chromatography (TLC). The crude product was recrystallized twice from methyl alcohol to give the refined product.

*3.3.5.1. Data for compound (**8a**).* 73.8% yield; obtained as a yellow solid; mp: 210–212 °C; other characteristics are similar with the literature we published before.[20]

*3.3.5.2. Data for compound (**8b**).* 68.2% yield; obtained as a yellow solid; IR (KBr) ν_{max} 3023, 2908, 1738, 1604, 1504, 1396, 1262, 1039, 750 cm^{-1}; ^{1}H NMR (400 MHz, DMSO-d_6): δ 9.88 (s, 1H), 9.07 (s, 1H), 8.34 (d, J = 9.3 Hz, 1H), 8.25 (d, J = 9.2 Hz, 1H), 8.19 (dd, J = 7.8, 1.8 Hz, 1H), 7.82 (d, J = 11.9 Hz, 1H), 7.77 (ddd, J = 9.0, 7.4, 1.8 Hz, 1H), 7.33 (d, J = 8.4 Hz, 1H), 7.20 (t, J = 7.6 Hz, 1H), 7.10 (s, 1H), 6.19 (s, 2H), 4.86–5.01 (m, 2H), 4.06 (d, J = 13.6 Hz, 3H), 3.93 (s, 3H), 3.13–3.24 (m, 2H); HR-ESI-MS: m/z 456.1997 $[M]^+$ (calcd for $C_{27}H_{22}NO_6$, 456.1442).

*3.3.5.3. Data for compound (**8c**).* 65.4% yield; obtained as a yellow solid; IR (KBr) ν_{max} 3009, 2846, 1748, 1614, 1504, 1395, 1274, 1207, 1103, 1035, 818, 764 cm^{-1}; ^{1}H NMR (400 MHz, DMSO-d_6) δ 9.94 (s, 1H), 9.10 (s, 1H), 8.31–8.40 (m, 1H), 8.27 (d, J = 9.2 Hz, 1H), 8.18 (d, J = 2.8 Hz, 1H), 7.85 (d, J = 3.1 Hz, 1H), 7.83 (d, J = 2.8 Hz, 1H), 7.39 (d, J = 9.1 Hz, 1H), 7.11 (s, 1H), 6.19 (s, 2H), 4.84–5.02 (m, 2H), 4.06 (d, J = 10.7 Hz, 3H), 3.94 (s, 3H), 3.20 (dd, J = 15.3, 9.0 Hz, 2H); HR-ESI-MS: m/z 490.1633 $[M]^+$ and m/z 492.1617 $[M + 2]^+$ (calcd for $C_{27}H_{21}ClNO_6$, 490.1052).

*3.3.5.4. Data for compound (**8d**).* 63.7% yield; obtained as a yellow solid; IR (KBr) ν_{max} 3404, 2904, 1750, 1613, 1505, 1394, 1276, 1207, 1102, 1034, 816, 621 cm^{-1}; ^{1}H NMR (500 MHz, DMSO-d_6) δ 9.93 (s, 1H), 9.07 (s, 1H), 8.34 (d, J = 9.1 Hz, 1H), 8.27 (d, J = 5.0 Hz, 1H), 8.26 (d, J = 9.2 Hz, 1H), 7.94 (d, J = 8.9 Hz, 1H), 7.82 (d, J = 2.7 Hz, 1H), 7.33 (d, J = 9.1 Hz, 1H), 7.11 (d, J = 7.4 Hz, 1H), 6.18 (d, J = 9.6 Hz, 2H), 4.92 (s, 2H), 4.02–4.09 (m, 3H), 3.93 (s, 3H), 3.21 (d, J = 6.1 Hz, 2H); HR-ESI-MS: m/z 534.1188 $[M]^+$ and m/z 536.1167 $[M + 2]^+$ (calcd for $C_{27}H_{21}BrNO_6$, 534.0547).

*3.3.5.5. Data for compound (**8e**).* 68.2% yield; obtained as a yellow solid; other characteristics are similar with the literature reported.[42]

*3.3.5.6. Data for compound (**8f**).* 60.8% yield; obtained as a yellow solid; IR (KBr) ν_{max} 3029, 2893, 1748, 1606, 1508, 1397, 1280, 1219, 1105, 1040, 759 cm^{-1}; ^1H NMR (400 MHz, DMSO-d_6) δ 9.88 (s, 1H), 9.08 (s, 1H), 8.34 (d, J = 9.3 Hz, 1H), 8.22–8.30 (m, 1H), 8.15–8.21 (m, 1H), 7.83 (d, J = 2.7, 1H), 7.73 (ddd, J = 8.9, 7.4, 1.8 Hz, 1H), 7.31 (d, J = 8.3 Hz, 1H), 7.18 (t, J = 7.5 Hz, 1H), 7.10 (s, 1H), 6.19 (d, J = 4.0 Hz, 2H), 4.87–5.00 (m, 2H), 4.20 (q, J = 6.9 Hz, 2H), 4.05 (s, 3H), 3.18–3.25 (m, 2H), 3.17 (s, 2H), 1.36 (t, J = 6.9 Hz, 3H); HR-ESI-MS: m/z 470.2158 $[M]^+$ (calcd for $C_{28}H_{24}NO_6$, 470.1598).

*3.3.5.7. Data for compound (**8g**).* 61.2% yield; obtained as a yellow solid; other characteristics are similar with the literature we published before.[21]

*3.3.5.8. Data for compound (**8h**).* 53.8% yield; obtained as a yellow solid; IR (KBr) ν_{max} 3426, 2953, 1763, 1614, 1506, 1396, 1278, 1226, 1125, 1068, 1039 cm^{-1}; ^1H NMR (500 MHz, DMSO-d_6) δ 9.97 (s, 1H), 9.10 (s, 1H), 8.41 (d, J = 8.4 Hz, 1H), 8.35 (d, J = 9.3 Hz, 1H), 8.26–8.30 (m, 1H), 7.81–7.87 (m, 1H), 7.70–7.75 (m, 1H), 7.68 (dd, J = 8.1, 1.9 Hz, 1H), 7.11 (s, 1H), 6.19 (s, 2H), 4.86–4.97 (m, 2H), 4.06 (d, J = 20.3 Hz, 3H), 3.21 (dd, J = 14.3, 8.1 Hz, 2H), 2.24 (s, 3H); HR-ESI-MS: m/z 518.0922 $[M]^+$ and m/z 520.0892 $[M + 2]^+$ (calcd for $C_{28}H_{21}ClNO_7$, 518.1001).

*3.3.5.9. Data for compound (**8i**).* 51.5% yield; obtained as a yellow solid; IR (KBr) ν_{max} 3385, 3019, 2842, 1738, 1604, 1504, 1395, 1262, 1214, 1135, 1103, 1037, 930, 758 cm^{-1}; ^1H NMR (500 MHz, DMSO-d_6) δ 9.99 (s, 1H), 9.07 (s, 1H), 8.39 (d, J = 2.6 Hz, 1H), 8.34 (d, J = 9.3 Hz, 1H), 8.27 (d, J = 9.2 Hz, 1H), 7.98 (dd, J = 8.7, 2.7 Hz, 1H), 7.83 (s, 1H), 7.51 (d, J = 8.7 Hz, 1H), 7.11 (s, 1H), 6.18 (d, J = 11.2 Hz, 2H), 4.86–4.96 (m, 2H), 3.99–4.12 (m, 3H), 3.19–3.25 (m, 2H), 2.20 (s, 3H); HR-ESI-MS: m/z 518.1614 $[M]^+$ and m/z 520.1600 $[M + 2]^+$ (calcd for $C_{28}H_{21}ClNO_7$, 518.1001).

*3.3.5.10. Data for compound (**8j**).* 53.7% yield; obtained as a yellow solid; IR (KBr) ν_{max} 3338, 3016, 1752, 1616, 1506, 1480, 1366, 1273, 1203, 1100, 1031, 920, 761 cm^{-1}; ^1H NMR (500 MHz, DMSO-d_6) δ 9.99 (s, 1H), 9.07 (s, 1H), 8.39 (d, J = 2.6 Hz, 1H), 8.34 (d, J = 9.3 Hz, 1H), 8.27 (d, J = 9.2 Hz, 1H), 7.98 (dd, J = 8.7, 2.7 Hz, 1H), 7.83 (s, 1H), 7.51 (d, J = 8.7 Hz, 1H), 7.11 (s, 1H), 6.19 (s, 2H), 4.83–5.01 (m, 2H), 4.04 (s, 3H), 3.17–3.27 (m, 2H), 2.25 (s, 3H); HR-ESI-MS: 562.1165 m/z $[M]^+$ and m/z 564.1152 $[M + 2]^+$ (calcd for $C_{28}H_{21}BrNO_7$, 562.0496 m/z).

*3.3.5.11. Data for compound (**8k**).* 59.1% yield; obtained as a yellow solid; IR (KBr) ν_{max} 3302, 3026, 2906, 1745, 1615, 1504, 1436, 1366, 1340, 1204, 1039, 822, 777 cm^{-1}; ^1H NMR (500 MHz, DMSO-d_6) δ 9.91 (s, 1H), 9.11 (s, 1H), 8.34 (d, J = 9.3 Hz, 1H), 8.29 (t, J = 5.4 Hz, 1H), 8.27 (d, J = 9.2 Hz, 1H), 7.84 (s, 1H), 7.41 (d, J = 8.0 Hz, 1H), 7.25 (s, 1H), 7.10 (s, 1H), 6.19 (s, 2H), 4.87–4.99 (m, 2H), 4.03 (s, 3H), 3.21 (dd, J = 13.2, 7.0 Hz, 2H), 2.48 (s, 3H), 2.22 (s, 3H); HR-ESI-MS: m/z 498.2134 $[M]^+$ (calcd for $C_{29}H_{24}NO_7$, 498.1547).

*3.3.5.12. Data for compound (**8l**).* 54.3% yield; obtained as a yellow solid; IR (KBr) ν_{max} 3340, 3033, 2904, 1744, 1618, 1504, 1440, 1366, 1340, 1275, 1186, 1033, 928, 822, 573 cm^{-1}; ^1H NMR (500 MHz, DMSO-d_6) δ 9.93 (d, J = 9.9 Hz, 1H), 9.11 (s, 1H), 8.33 (t, J = 11.6 Hz, 1H), 8.23–8.31 (m, 1H), 8.21 (t, J = 6.9 Hz, 1H), 7.83 (d, J = 16.3 Hz, 1H), 7.68 (dd, J = 8.3, 1.9 Hz, 1H), 7.29 (t, J = 8.9 Hz, 1H), 7.12 (d, J = 17.6 Hz, 1H), 6.21 (d, J = 12.2 Hz, 2H), 4.87–5.02 (m, 2H), 4.04 (s, 3H), 3.21 (dd, J = 13.7, 7.6 Hz, 2H), 2.47 (s, 3H), 2.21 (s, 3H); HR-ESI-MS: m/z 498.2138 $[M]^+$ (calcd for $C_{29}H_{24}NO_7$, 498.1547).

*3.3.5.13. Data for compound (**8m**).* 58.3% yield; obtained as a yellow solid; IR (KBr) ν_{max} 3308, 2986, 1749, 1603, 1514, 1367, 1278, 1208, 1036, 779 cm^{-1}; ^1H NMR (500 MHz, DMSO-d_6) δ 10.02 (s, 1H), 9.07 (d, J = 8.5 Hz, 1H), 8.36 (d, J = 9.3 Hz, 1H), 8.30–8.34 (m, 2H), 8.27 (d, J = 9.2 Hz, 1H), 7.83 (d, J = 2.6 Hz, 1H), 7.43–7.52 (m, 2H), 7.10 (s, 1H), 6.19 (d, J = 5.4 Hz, 2H), 4.86–4.96 (m, 2H), 4.03 (s, 3H), 3.18–3.24 (m, 2H), 2.36 (s, 3H); HR-ESI-MS: m/z 484.0838 $[M]^+$ (calcd for $C_{28}H_{22}NO_7$, 484.1391).

*3.3.5.14. Data for compound (**8n**).* 49.8% yield; obtained as a yellow solid; IR (KBr) ν_{max} 3419, 2980, 2943, 2906, 1740, 1603, 1504, 1399, 1373, 1334, 1279, 1231, 1122, 1034 cm^{-1}; ^1H NMR (500 MHz, DMSO-d_6): δ 9.97 (s, 1H), 9.09 (s, 1H), 8.33 (d, J = 9.3 Hz, 1H), 8.26–8.31 (m, 1H), 7.83 (s, 1H), 7.54 (s, 2H), 7.11 (s, 1H), 6.18 (s, 2H), 4.86–4.98 (m, 2H), 4.00–4.09 (m, 3H), 3.93 (d, J = 8.0 Hz, 6H), 3.83 (s, 3H), 3.17–3.25 (m, 2H); HR-ESI-MS: m/z 516.2278 $[M]^+$ (calcd for $C_{29}H_{26}NO_8$, 516.1653).

*3.3.5.15. Data for compound (**8o**).* 40.6% yield; obtained as a yellow solid; IR (KBr) ν_{max} 3403, 2890, 1768, 1608, 1505, 1395, 1370, 1324, 1277, 1221, 1106, 1060 cm^{-1}; ^1H NMR (500 MHz, DMSO-d_6): δ 9.97 (s, 1H), 9.09 (s, 1H), 8.35 (d, J = 9.3 Hz, 1H), 8.27 (d, J = 9.2 Hz, 1H), 7.84 (s, 1H), 7.50 (s, 2H), 7.11 (s, 1H), 6.20 (s, 2H), 4.86–4.99 (m, 2H), 4.07–4.31 (m, 6H), 4.04 (s, 3H), 3.14–3.26 (m, 2H), 1.40 (t, J = 6.9 Hz, 6H), 1.25–1.35 (m, 3H); HR-ESI-MS: m/z 558.2906 $[M]^+$ (calcd for $C_{32}H_{32}NO_8$, 558.2122).

*3.3.5.16. Data for compound (**8p**).* 48.0% yield; obtained as a yellow solid; IR (KBr) ν_{max} 3403, 2890, 1768, 1608, 1505, 1395, 1370, 1324, 1277, 1221, 1160, 1060 cm^{-1}; ^1H NMR (500 MHz, DMSO-d_6): δ 10.07 (s, 1H), 9.08 (s, 1H), 8.36 (d, J = 9.4 Hz, 1H), 8.27–8.30 (m, 1H), 8.12 (s, 2H), 7.84 (s, 1H), 7.10 (d, J = 2.8 Hz, 1H), 6.19 (s, 2H), 4.87–4.92 (m, 2H), 4.05 (d, J = 3.5 Hz, 3H), 3.19–3.23 (m, 2H), 2.40 (s, 3H), 2.35 (s, 6H); HR-ESI-MS: m/z: 600.3245 $[M]^+$ (calcd for $C_{32}H_{26}NO_{11}$, 600.1500).

3.4. The calculation of the partition coefficient (log *P*)

The partition coefficient, abbreviated as P, is defined as a particular distribution ratio of molecules in oil and water, and is useful in predicting the absorption of drugs within the body. Hence, the log P is a criterion used in decision-making by medicinal chemists in pre-clinical drug discovery. To investigate the druggability of berberine derivatives, log P of **BBR** and its derivatives were calculated using ALOGPS 2.1 software.

3.5. Antioxidant activity assays

The antioxidant activities of berberine derivatives **8a–8p** were measured by FRAP, ABTS, DPPH and HOSC assays. IC_{50} was calculated by means of SPSS Statistics 21 software. A significant difference is considered at the level of $p < 0.05$.

3.5.1. ABTS assay. The ABTS assay is a widely applied method for measuring the radical-scavenging ability of antioxidants. ABTS can be oxidized to green $ABTS^{\bullet+}$ (maximum

absorbance at 734 nm) under the action of an oxidant, and the generation of $ABTS^{\cdot+}$ can be inhibited by an antioxidant. The assay was carried out according to a previously reported method.[43] Generally, the $ABTS^{\cdot+}$ aqueous mother solution was prepared by mixing the ABTS solution and oxidant, and stored in the dark at room temperature for 12–16 h. Aliquots containing 10 μL of different concentrations of sample in DMSO were added to 200 μL $ABTS^{\cdot+}$ solution ($A_{734\ nm} = 0.700 \pm 0.02$) ($A_x$) by dilution of the $ABTS^{\cdot+}$ aqueous mother solution with ethanol (20% of water). Methanol was set as the blank (A_0), and different concentrations of assays were set as the control (A_{x0}). The absorbance was read every 20 s at 30 °C in 6 min by ELISA. The radical scavenging activity in percentage (RSA%) was calculated according to Nanjappa *et al.*,[44] with some modifications as described in the equation below:

$$\mathrm{RSA\%} = 1 - \frac{A_x - A_{x0}}{A_0} \times 100\%$$

3.5.2. DPPH assay. Radical scavenging efficiencies of the compounds were evaluated by DPPH analysis. DPPH, a kind of stable radical, with absorption at 517 nm, can be paired with a free radical scavenger, generating a pale yellow non-radical form (DPPH-H), which has no absorption at 517 nm. The DPPH radical solution was prepared by dissolving 1 mg of DPPH in 20 mL of methanol and stored in the dark. 1.5 mL DPPH and 1 mL different concentrations of the sample dissolved in DMSO were mixed (A_x), shaken and reacted in the dark for 30 min. The mixture containing 1.5 mL DPPH and 1 mL DMSO was used as a negative control (A_0), the referrals anti-oxidant (ascorbic acid) in methanol and DPPH radical solution were set as positive controls. Furthermore, mixture of 1.5 mL methanol and 1 mL sample was measured as background signal (A_{x0}). All measurements were carried out in triplicate. The decrease of the absorbance of the compound mixture at 517 nm represented the capability of the samples. The radical scavenging activity in percentage (RSA%) was determined according to Mensor *et al.*,[45,46] with some modifications as described in the equation below:

$$\mathrm{RSA\%} = 1 - \frac{A_x - A_{x0}}{A_0} \times 100\%$$

3.5.3. HOSC assay. The hydroxyl radical (·OH) scavenging effects of the synthesized compounds were examined. Generation of ·OH was carried out through the Fenton reaction by mixing H_2O_2 and Fe(II) with salicylic acid.[47,48] The reaction system contained 1 mL of 9 mM $FeSO_4$ and 1 mL of 9 mM salicylic acid dissolved in ethanol and 1 mL of various concentrations of samples. The reaction system was freshly prepared and reacted at 37 °C for 30 min prior to the detection of absorbance at 510 nm (A_x). Two controls were applied for this test: deionized water was set as a negative control (blank) (A_0). To avoid the disturbance of color, the reaction system without the addition of H_2O_2 was set as the control (A_{x0}). Each value is presented as the average of three determinations. The hydroxyl radical scavenging activity (HRSA%) was calculated. The equation is shown below:

$$\mathrm{HOSA\%} = 1 - \frac{A_x - A_{x0}}{A_0} \times 100\%$$

3.5.4. Ferric reducing antioxidant power (FRAP) assay. The principle of FRAP is that antioxidants can restore ferric-tripyridyltriazine (TPTZ-Fe(III)) in acidic conditions, and generate the stable ferrous form (TPTZ-Fe(II)), which has the maximum absorbance wavelength at 593 nm, and then the antioxidant potential of the compounds was estimated according to the absorbance. The FRAP assay was carried out in accordance with the previous literature.[49] Briefly, 10 mM TPTZ was dissolved in 40 mM hydrochloric acid (HCl), 20 mM $FeCl_3 \cdot 6H_2O$, 0.3 M acetate buffer to a final pH of 3.6, and different concentrations of the sample and $FeSO_4 \cdot 6H_2O$ (1.25, 2.5, 5, 25, 100, 150, 200, 400, 500 μM) were prepared. 1.9 mL FRAP reagent containing TPTZ, $FeCl_3 \cdot 6H_2O$ and acetate buffer according to the proportion of 10 : 1 : 1 with 100 μL sample were mixed. Before reading the absorbance at 595 nm by ELISA, the mixture was shaken and reacted at 37 °C for 30 min. Iron(II) sulfate solution was used for calibration. The FRAP values are expressed as concentrations of iron(II). All analyses were done in triplicate.

3.6. Comprehensive analysis of the antioxidant activity using a color grading profile

To comprehensively understand the antioxidant activities of these **BBR** derivatives, we compared their activities with **BBR** by comprehensive analysis of the antioxidant activities from ABTS, DPPH, HOSC, and FRAP assays. The compounds with superior activities were labeled with red color, the compounds with inferior activities were labeled with green color, and the compounds with equal activities to **BBR** were labeled with white color. The darkness of the color indicated the degree of superiority and inferiority. The final results are presented using the mixed color of the four colors that resulted from ABTS, DPPH, HOSC and FRAP assays to indicate the antioxidant activities.

3.7. The molecular electric potentials (MEPs)

The molecular electric potentials (MEPs) of berberine and compound **8p** were analyzed. The optimized structures are characterized as minima by means of vibrational analysis using ChemBio3D Ultra 14.0. Density functional theory (DFT/B3LYP) at the 3-21G (d,p) was used to calculate the MEPs, and the calculation was performed using the Gaussian 09W program package with default convergence. The MEPs of compounds on the electron density distribution were plotted with GaussView, and were presented by a color code ranging from 0.05 to 0.143 hartree.

Conflicts of interest

There are no conflicts to declare.

Acknowledgements

This work was financially supported by the Huxiang Young Talent Support Program of Hunan Province (2018RS3005), the Innovation-Driven Project of Central South University (2020CX048), the Changsha Science and Technology Plan Project (kq2005001, kq2004086), the National Natural Science Foundation of China (81301258), the Natural Science Foundation of Hunan Province (2019JJ60071, 2020JJ4680), the Shenghua Yuying Project of Central South University, the Postgraduate Innovation Project of Central South University (2020zzts819, 2020zzts408 and 2020zzts409), and the Open-End Fund for the Valuable and Precision Instruments of Central South University.

References

1 Y. P. Li, H. Wu and L. M. Du, *Chin. Chem. Lett.*, 2009, **20**, 322–325.
2 A. Poudel, J. Y. Zhou, N. Mekala, R. Welchko, M. G. Rosca and L. X. Li, *Can. J. Physiol. Pharmacol.*, 2019, **97**, 699–707.
3 X. L. Ma, Z. J. Chen, L. Wang, G. S. Wang, Z. H. Wang, X. B. Dong, B. Y. Wen and Z. C. Zhang, *Front. Pharmacol.*, 2018, **9**, 13.
4 A. W. Feng, C. Yu, Q. Mao, N. Li, Q. R. Li and J. S. Li, *Fitoterapia*, 2011, **82**, 976–982.
5 Y. He, X. Yuan, G. Zhou and A. Feng, *Fitoterapia*, 2018, **124**, 200–205.
6 Y. H. Ma, M. Y. Wei, Y. Y. Liu, F. R. Song, Z. Y. Liu and Z. F. Pi, *Chin. Chem. Lett.*, 2016, **27**, 215–220.
7 M. Javadipour, M. Rezaei, E. Keshtzar and M. J. Khodayar, *J. Biochem. Mol. Toxicol.*, 2019, **33**, e22368.
8 N. Erol, L. Saglam, Y. S. Saglam, H. S. Erol, S. Altun, M. S. Aktas and M. B. Halici, *Inflammation*, 2019, **42**, 1585–1594.
9 C. Y. Chuang, H. C. Liu, L. C. Wu, C. Y. Chen, J. H. T. Chang and S. L. Hsu, *J. Agric. Food Chem.*, 2010, **58**, 2943–2951.
10 A. V. Snezhkina, A. V. Kudryavtseva, O. L. Kardymon, M. V. Savvateeva, N. V. Melnikova, G. S. Krasnov and A. A. Dmitriev, *Oxid. Med. Cell. Longevity*, 2019, **2019**, 6175804.
11 Y. Wu, M. Chen and J. Jiang, *Mitochondrion*, 2019, **49**, 35–45.
12 A. Gonzalez-Sarrias, M. A. Nunez-Sanchez, F. A. Tomas-Barberan and J. C. Espin, *J. Agric. Food Chem.*, 2017, **65**, 752–758.
13 S. Wyck, C. Herrera, C. E. Requena, L. Bittner, P. Hajkova, H. Bollwein and R. Santoro, *Epigenet. Chromatin*, 2018, **11**, 17.
14 C. Liu, Y. T. Fu, C. E. Li, T. F. Chen and X. L. Li, *J. Agric. Food Chem.*, 2017, **65**, 4405–4413.
15 J. Y. Zhou and S. W. Zhou, *Fitoterapia*, 2011, **82**, 184–189.
16 X. J. Cui, Y. Y. Lu, M. Zhao, S. Qian and Y. Wu, *Chin. Chem. Lett.*, 2010, **21**, 1281–1282.
17 B. Mistry, Y. S. Keum and D. H. Kim, *Res. Chem. Intermed.*, 2016, **42**, 3241–3256.
18 B. Mistry, R. V. Patel, Y. S. Keum and D. H. Kim, *Saudi J. Biol. Sci.*, 2017, **24**, 36–44.
19 B. M. Mistry, H. S. Shin, Y. S. Keum, M. Pandurangan, D. H. Kim, S. H. Moon, A. A. Kadam, S. K. Shinde and R. V. Patel, *Anti-Cancer Agents Med. Chem.*, 2017, **17**, 1652–1660.
20 S. S. Zhang, X. H. Wang, W. C. Yin, Z. B. Liu, M. Zhou, D. P. Xiao, Y. F. Liu and D. M. Peng, *Bioorg. Med. Chem. Lett.*, 2016, **26**, 4799–4803.
21 Z. B. Liu, X. H. Wang, H. Zhang, S. S. Zhang, Y. Q. Li, Y. F. Liu and D. M. Peng, *Med. Chem. Res.*, 2017, **26**, 672–679.
22 Y. Zhong, C.-M. Ma and F. Shahidi, *J. Funct. Foods*, 2012, **4**, 87–93.
23 V. S. Pilyugin, Y. E. Sapozhnikov and N. A. Sapozhnikova, *Russ. J. Gen. Chem.*, 2004, **74**, 738–743.
24 D. P. Xiao, F. He, D. M. Peng, M. Zou, J. Y. Peng, P. Liu, Y. F. Liu and Z. B. Liu, *Anti-Cancer Agents Med. Chem.*, 2018, **18**, 1639–1648.
25 C. S. Liu, Y. R. Zheng, Y. F. Zhang and X. Y. Long, *Fitoterapia*, 2016, **109**, 274–282.
26 E. S. Lima, A. C. S. Pinto, K. L. Nogueira, L. Silva, P. D. O. de Almeida, M. C. de Vasconcellos, F. C. M. Chaves, W. P. Tadei and A. M. Pohlit, *Molecules*, 2013, **18**, 178–189.
27 G. Aldini, A. Altomare, G. Baron, G. Vistoli, M. Carini, L. Borsani and F. Sergio, *Free Radical Res.*, 2018, **52**, 751–762.
28 A. Dominari, D. Hathaway III, A. Kapasi, T. Paul, S. S. Makkar, V. Castaneda, S. Gara, B. M. Singh, K. Agadi and M. Butt, *World J. Virol.*, 2021, **10**, 34–52.
29 A. Nagy, F. Vanderbist, N. Parij, P. Maes, P. Fondu and J. Neve, *Pulm. Pharmacol. Ther.*, 1997, **10**, 287–292.
30 Y. Yang, L. Li, Q. Hang, Y. Fang, X. Dong, P. Cao, Z. Yin and L. Luo, *Redox Biol.*, 2019, **20**, 157–166.
31 M. H. Zarka and W. J. Bridge, *Redox Biol.*, 2017, **11**, 631–636.
32 L. József and J. G. Filep, *Free Radical Biol. Med.*, 2003, **35**, 1018–1027.
33 H. Sies and M. J. Parnham, *Free Radical Biol. Med.*, 2020, **156**, 107–112.
34 K. K. Dong, N. Damaghi, J. Kibitel, M. T. Canning, K. A. Smiles and D. B. Yarosh, *J. Cosmet. Dermatol.*, 2007, **6**, 183–188.
35 A. Abdelwahed, I. Bouhlel, I. Skandrani, K. Valenti, M. Kadri, P. Guiraud, R. Steiman, A.-M. Mariotte, K. Ghedira and F. Laporte, *Chem. Biol. Interact.*, 2007, **165**, 1–13.
36 X. N. Li, L. Y. Ma, H. Ji, Y. H. Qin, S. S. Jin and L. X. Xu, *Exp. Ther. Med.*, 2018, **16**, 4339–4348.
37 W. Y. Oh and F. Shahidi, *Food Chem.*, 2018, **261**, 267–273.
38 J.-M. Hwang, C.-J. Wang, F.-P. Chou, T.-H. Tseng, Y.-S. Hsieh, W.-L. Lin and C.-Y. Chu, *Arch. Toxicol.*, 2002, **76**, 664–670.
39 M. H. Jang, H. Y. Kim, K. S. Kang, T. Yokozawa and J. H. Park, *Arch. Pharmacal Res.*, 2009, **32**, 341–345.
40 P. Li, S. Liao, J. Wang, D. Xu, Q. Zhang, M. Yang and L. Kong, *RSC Adv.*, 2016, **6**, 47474–47485.
41 A. Shirwaikar, A. Shirwaikar, K. Rajendran and I. S. R. Punitha, *Biol. Pharm. Bull.*, 2006, **29**, 1906–1910.
42 H. S. Bodiwala, S. Sabde, D. Mitra, K. K. Bhutani and I. P. Singh, *Eur. J. Med. Chem.*, 2011, **46**, 1045–1049.
43 C. H. Jeong, G. N. Choi, J. H. Kim, J. H. Kwak, D. O. Kim, Y. J. Kim and H. J. Heo, *Food Chem.*, 2010, **118**, 278–282.
44 C. Nanjappa, S. K. T. Hanumanthappa, G. Nagendrappa, P. S. S. Ganapathy, S. D. Shruthi, S. S. More, G. Jose,

H. B. V. Sowmya and R. S. Kulkarni, *Synth. Commun.*, 2015, **45**, 2529–2545.

45 L. L. Mensor, F. S. Menezes, G. G. Leitao, A. S. Reis, T. C. dos Santos, C. S. Coube and S. G. Leitao, *Phytother. Res.*, 2001, **15**, 127–130.

46 I. Lakkab, H. El Hajaji, N. Lachkar, R. Lefter, A. Ciobica, B. El Bali and M. Lachkar, *J. Funct. Foods*, 2019, **54**, 457–465.

47 J. Moore, J. J. Yin and L. L. Yu, *J. Agric. Food Chem.*, 2006, **54**, 617–626.

48 A. Sannasimuthu and J. Arockiaraj, *J. Funct. Foods*, 2019, **61**, 103513.

49 M. Trujillo, E. Gallardo, A. Madrona, L. Bravo, B. Sarria, J. A. Gonzalez-Correa, R. Mateos and J. L. Espartero, *J. Agric. Food Chem.*, 2014, **62**, 10297–10303.